JOURNAL OF NATURAL PRODUCTS

Article

pubs.acs.org/jnp

Antibacterial Labdane Diterpenoids from *Vitex vestita*

Nina Corlay,[†] Marylin Lecsö-Bornet,[‡] Erell Leborgne,[†] Florent Blanchard,[†] Xavier Cachet,[†,§] Jérôme Bignon,[†] Fanny Roussi,[†] Marie-Jose Butel,[‡] Khalijah Awang,[∥] and Marc Litaudon*[,†]

[†]Centre de Recherche de Gif, LabEx CEBA, Institut de Chimie des Substances Naturelles (ICSN), CNRS UPR 2301, 91198 Gif-sur-Yvette, France

[‡]Laboratoire Ecosystème Intestinal, Probiotiques, Antibiotiques-EA 4065 and [§]Laboratoire de Pharmacognosie, UMR 8638 COMETE CNRS, Université Paris Descartes, Sorbonne Paris Cité, Faculté de Pharmacie, 75006 Paris, France

[∥]Department of Chemistry, University Malaya, 59100 Kuala Lumpur, Malaysia

Supporting Information

ABSTRACT: A large-scale in vitro screening of tropical plants using an antibacterial assay permitted the selection of several species with significant antibacterial activities. Bioassay-guided purification of the dichloromethane extract of the leaves of the Malaysian species *Vitex vestita*, led to the isolation of six new labdane-type diterpenoids, namely, 12-epivitexolide A (**2**), vitexolides B and C (**3** and **4**), vitexolide E (**8**), and vitexolins A and B (**5** and **6**), along with six known compounds, vitexolides A (**1**) and D (**7**), acuminolide (**9**), 3β-hydroxyanticopalic acid (**10**), 8α-hydroxyanticopalic acid (**11**), and 6α-hydroxyanticopalic acid (**12**). Their structures were elucidated on the basis of 1D and 2D NMR analyses and HRMS experiments. Both variable-temperature NMR spectroscopic studies and chemical modifications were performed to investigate the dynamic epimerization of the γ-hydroxybutenolide moiety of compounds **1**−**4**. Compounds were assayed against a panel of 46 Gram-positive strains. Vitexolide A (**1**) exhibited the most potent antibacterial activity with minimal inhibitory concentration values ranging from 6 to 96 μM, whereas compounds **2** and **6**−**9** showed moderate antibacterial activity. The presence of a β-hydroxyalkyl-γ-hydroxybutenolide subunit contributed significantly to antibacterial activity. Compounds **1**−**4** and **6**−**9** showed cytotoxic activities against the HCT-116 cancer cell line ($1 < IC_{50}s < 10$ μM) and human fetal lung fibroblast MRC5 cell line ($1 < IC_{50}s < 10$ μM for compounds **1**, **2**, **7**, **8**, and **9**).

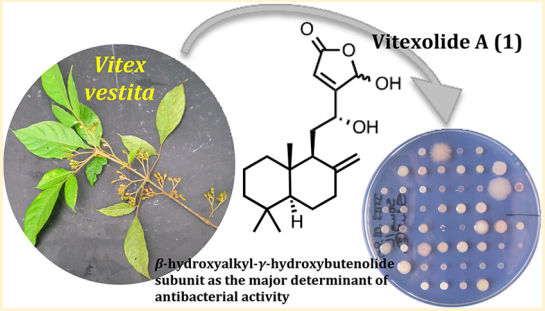

In recent decades, bacterial resistance to antibiotics became a serious and ongoing concern. In light of the emergence of multidrug resistance in common pathogens, discovering new antibacterial agents is a huge challenge. In the past, natural products played an essential role in antibiotic drug development and still offer significant potential for the discovery of novel antibacterial therapies. Through the diversity of their structures, they represent a rich source of inspiration to identify novel scaffolds for the development of new classes of antibiotics with novel mechanisms of action. Approximately 1400 MeOH and CH_2Cl_2 extracts of 476 tropical plant species were tested in a preliminary biological screening for their antimicrobial activity against 49 bacterial strains representing 41 species (15 Gram-positive and 26 Gram-negative). This led to the selection of *Vitex vestita* (Lamiaceae) for further chemical investigation.

Vitex vestita is a 1−5 m tall shrub widely distributed throughout southeast Asia (Borneo, Sumatra, Burma, Vietnam, and China).[1] The use of *Vitex* species in folk medicine in Asia and Europe is quite common, especially for treatment of female hormonal disorders (*V. agnus castus*), headache (*V. rotundifolia* and *V. trifolia*), and bacterial dysentery and diarrhea (*V. agnus castus* and *V. rotundifolia*).[2] Recently, Kannathasan and co-workers reported the in vitro antibacterial potential of several Indian *Vitex* species against various human pathogenic bacteria.[3] Plants of the genus *Vitex* are known to produce various labdane-type diterpenoids, many of them possessing a tetrahydrofuran or a γ-lactone moiety on the side chain.[4−7] Some of them, endowed with interesting biological properties, are promising compounds for various medical applications, such as selective inhibitors of NO production, TAF antagonists, α-glucosidase inhibitors, and/or cytotoxic agents.[8] Thus, far, only one study dealing with the hepatoprotective activity of crude extracts from *Vitex vestita* roots has been reported.[9] The following study represents the first chemical investigation of this species. In this paper, we report the bioassay-guided isolation, structural elucidation, and both the antibacterial and cytotoxic activities of six new (**2**−**6** and **8**) and six known (**1**, **7**, and **9**−**12**) labdane derivatives. Compounds **1** and **7**, which were previously obtained by chemical synthesis,[10,11] are identified as natural products for the first time.

Received: March 6, 2015
Published: June 2, 2015

DOI: 10.1021/acs.jnatprod.5b00206
J. Nat. Prod. 2015, 78, 1348−1356

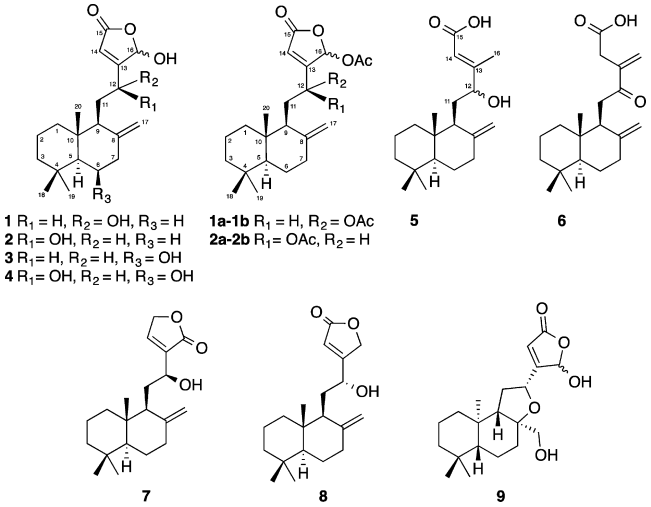

RESULTS AND DISCUSSION

In the primary biological screening, 6 extracts out of 1392 were shown to have significant antibacterial activities, defined as inhibition of several bacterial species and/or one pathogen species at a concentration of 60 mg/L. Among these, the CH_2Cl_2 extract from the leaves of *V. vestita* Wall. ex Schauer attracted our attention as it fully inhibited the bacterial growth of five *Enterococcus* spp. (*E. casseliflavus*, *E. hirae*, *E. gallinarum*, *E. faecium*, and *E. faecalis*), three *Bacillus* spp. (*B. cereus*, *B. subtilis*, and *B. pumilus*), three *Staphylococcus* spp. (*S. epidermidis*, *S. aureus*, and *S. lugdunensis*), *Streptococcus agalactiae*, and *Mycobacterium smegmatis*. The leaves (480 g) of this species were extracted with CH_2Cl_2 to give 14.1 g of crude extract, and 7 g of the latter was subjected to flash chromatography on silica gel to afford 16 fractions. Their antibacterial activities were evaluated against the same panel as the parent crude extract. Fraction 9 (2.25 g) exhibited the most effective antibacterial activity with 13 Gram-positive strains fully inhibited but no activity on Gram-negative strains. Subsequent flash chromatography on silica gel followed by preparative and analytical HPLC afforded the new vitexolides B, C, and E (**3**, **4**, and **8**, respectively) and 12-epivitexolide A (**2**) as well as the known vitexolides A and D (**1** and **7**, respectively), vitexolins A and B (**5** and **6**, respectively) along with acuminolide[12,13] (**9**), 3β-hydroxyanticopalic acid[14] (**10**), 8α-hydroxyanticopalic acid[15] (**11**), and 6α-hydroxyanticopalic acid[16] (**12**).

The ^{1}H and ^{13}C NMR data of compounds **1**–**8** (Tables 2–4) exhibited characteristic signals of a labdane-type structure including three methyls and an *exo*-methylene group. The presence of a *trans*-decalin core, as depicted in Figure 1, was highlighted from the following. Two spin systems A and B, involving protons from H1 to H3 and from H5 to H9, respectively, were identified by analysis of ^{1}H–^{1}H correlations

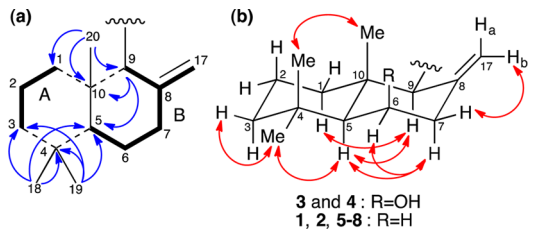

Figure 1. Key COSY (bold), HMBC (blue), and ROESY (red) correlations of the *trans*-decalin core of compounds **1**–**8**.

observed in the COSY spectrum. HMBC correlations from methyl groups 18 and 19 to C3, C4, and C5, and from $CH_3$20 to C1, C9, and C10 supported the location of the *gem*-dimethyl on C4 and a methyl group at C10. These correlations established the junction between the two spin systems A and B. Observed HMBC correlations from H9 to C5 and C10 confirmed that compounds **1**–**8** shared the same decalin moiety. In the ROESY data (Figure 1b), the presence of cross peaks between H5 and H9 on the one hand and between $CH_3$20 and $CH_3$18 on the other suggested the chair–chair conformation of the *trans*-decalin assembly.

Vitexolides A–C (**1**, **3**, and **4**) and 12-epivitexolide A (**2**) exhibited similar IR spectra consistent with the presence of an exomethylene group (2940 and 890 cm^{-1}), an α,β-unsaturated γ-lactone (1750 and 1640 cm^{-1}) moiety, and free hydroxy groups (3350 cm^{-1}). The construction of the side chain of compounds **1**–**4**, as depicted in Figure 2, was determined from

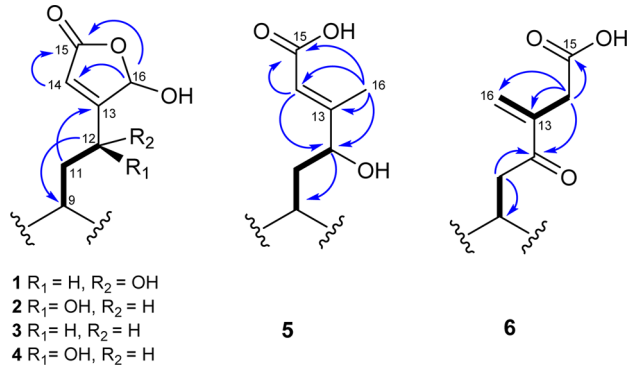

Figure 2. Key COSY (bold) and HMBC (blue) correlations of the side chains of compounds **1**–**6**.

analysis of 1D and 2D NMR data. Their ^{13}C NMR spectra showed two olefinic carbons at ca. δ_C 118 (C14) and 171 (C13), a carbonyl carbon at ca. δ_C 172 (broad, C15), and a hemiacetal carbon at ca. δ_C 98 (C16), which suggested the presence of a γ-hydroxybutenolide group. The *trans*-decalin and hydroxybutenolide moieties are connected by a two-carbon aliphatic chain as supported by HMBC correlations from $H_2$11 to C13 and H12 to C9. An interesting and common feature of the ^{1}H and ^{13}C NMR spectra of compounds **1**–**4** was the doubling (or broadening) of some signals when spectra were acquired at 298 K, which probably arises from either the existence of C16 epimers or/and conformational equilibrium rather than from a dynamic tautomeric equilibrium between epimers.[17−19] In the ^{1}H NMR spectra of compounds **1**–**4** acquired at a lower temperature of 263 K in acetone-d_6, some signals, particularly those of the β-hydroxyalkyl-γ-hydroxybutenolide subunit, were clearly duplicated (Table 2). In contrast, their coalescence into a broad signal was observed at 313 K. The two sets of signals observed at 263 K correspond to two epimeric forms in their favored conformation. These observations are evidence for the existence, under normal NMR conditions, of C16 epimers, and this was further confirmed by acetylation of compounds **1** and **2**, which allowed separation of both epimers as their corresponding diacetates (see below).

The HRESIMS data of vitexolides A and B (**1** and **3**) and 12-epivitexolide A (**2**) were all identical and in accordance with a molecular formula of $C_{20}H_{30}O_4$. Six indices of hydrogen deficiency can be deduced. Vitexolide A (**1**) was isolated as a

DOI: 10.1021/acs.jnatprod.5b00206
J. Nat. Prod. 2015, 78, 1348−1356

white powder. This compound was recently identified as a synthetic byproduct, named hydroxubutenolide-19, during the synthesis of zerumin B.[10] Prior to this, it had never been obtained from a natural source. It should be noted that the value of the chemical shift of C13 reported for the synthetic hydroxybutenolide-19[10] (i.e., δ_C 131.3) is erroneous. The actual value is δ_C 171.1, which is consistent with literature data reported for related compounds.[16,20] Furthermore, because the complete assignment of ^{1}H and ^{13}C NMR spectra has not been published, full NMR data of compound **1** are indicated in Tables 2 and 3. These ^{1}H and ^{13}C NMR data were similar to those of zerumin B, isolated from *Alpinia zerumbet*,[21] with the exception of the chemical shifts of olefinic carbons C13 and C14 and proton H14 (δ_C 171.1 and 118.1 and δ_H 6.05 for vitexolide A (**1**); δ_C 142.8 and 145.0 and δ_H 7.13 for zerumin B). The former ^{1}H and ^{13}C NMR resonances are typical of a β-alkyl-γ-hydroxybutenolide subunit,[20] whereas the latter correspond to an α-substituted one. Thus, vitexolide A (**1**) was established as a regioisomer of zerumin B. Thin needle-like crystals of one epimer of **1** were obtained from a 10:1 solution of MeOH/H_2O at room temperature. Such selective crystallization of only one epimer was also reported for dysidiolide.[18] The X-ray diffraction analysis of these crystals allowed the absolute configuration of one epimer of compound **1** to be assigned as 5*S*, 9*S*, 10*S*, 12*R*, 16*S* (ORTEP view is shown in Figure 3).

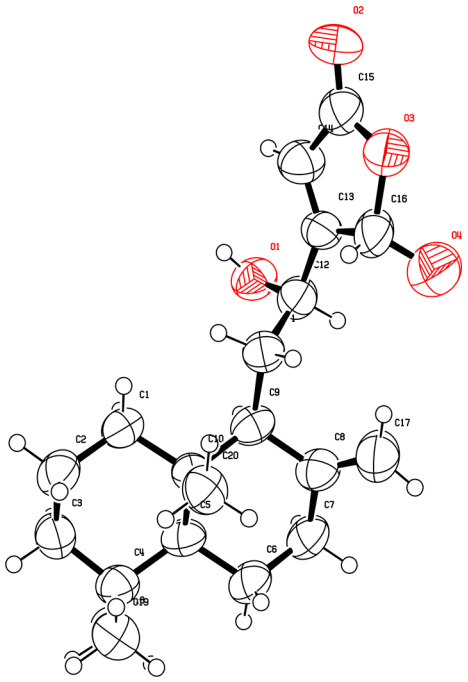

Figure 3. ORTEP view of the X-ray analysis of the 16*S* epimer of vitexolide A (**1**).

Compound **2** was isolated as colorless oil. Its NMR data were similar to those of **1**, except for the chemical shifts of H9 (δ_H 1.88 vs 2.25 for **1**) and $H_2$11 (δ_H 1.88 and 2.08 vs 1.69 and 1.90 for **1**), suggesting that compound **2** was the C12 epimer of vitexolide A. Similar differences have also been reported between zerumin B and 12-epizerumin B.[11] From these observations, compound **2** was identified as 12-epivitexolide A, and the 5*S*, 9*S*, 10*S*, 12*S*, absolute configuration was assigned to this compound.

With the aim to determine the ratio of the two C16 epimers, compounds **1** and **2** were subjected to acetylation. The acetylation of **1** yielded a C16 epimeric mixture of 12,16-diacetylated compounds **1a**,**b** in a 2:1 ratio, as determined by ^{1}H NMR spectroscopy. This is evidence that conformational constraints favored one epimer (**1a**). In contrast, the acetylation of **2** afforded an equimolar ratio of two 12,16-diacetylated derivatives **2a**,**b**. The purification of acetylated compounds by analytical HPLC did not affect the respective ratios because the acetylation inhibits epimerization at C16. The ^{1}H NMR data and specific rotation of compounds **1a**,**b** and **2a**,**b** are reported in Table 1. However, the C16 configuration of each compound could not be determined. ^{1}H and ^{13}C NMR data, respectively, for compounds **1**−**4** and **8** are included in Tables 2 and 3.

Table 1. Chemical Shifts of Key Protons of Compounds 1a,b and 2a,b ($CDCl_3$, 600 MHz, 298 K) and Their Specific Rotations (*c* 0.06, $CHCl_3$)

cpd	δ H16	δ H14	δ H12	δ $H_2$17	δ OAc (×2)	$[\alpha]^{25}_D$
1a	6.95 s	6.02 s	5.62 br d (*J* = 10.2 Hz)	4.86 s	2.17 s	+ 42
				4.30 s	2.11 s	
1b	7.00 s	6.10 s	5.41 br d (*J* = 10.4 Hz)	4.86 s	2.14 s	+13
				4.38 s	2.06 s	
2a	6.91 s	6.00 s	5.81 dd (*J* = 10.0, 5.0 Hz)	4.92 s	2.16 s	−2
				4.73 s	2.08 s	
2b	7.01 s	6.17 s	5.46 dd (*J* = 10.2, 5.0 Hz)	4.88 s	2.12 s	−10
				4.62 s	2.03 s	

Vitexolide B (**3**) was obtained as a white powder. Its ^{1}H NMR spectrum exhibited a pattern similar to those of compounds **1** and **2**. However, signals for methyl groups 18−20 appeared more deshielded than in **1** and **2**, suggesting that a hydroxy group was located on the bicyclic moiety rather than on the two-carbon aliphatic side chain connecting the γ-hydroxybutenolide unit. The COSY correlation observed from the oxymethine proton H6 (δ_H 4.42) to H7α (δ_H 2.30) confirmed its location at C6. In the ROESY spectrum, correlations between OH6 and $CH_3$18 and $CH_3$20 indicated the β-orientation of the hydroxy group. Thus, the relative configuration of compound **3** can be established as 5*S**, 6*R**,9*S**,10*R**. The specific rotation value of **3** (i.e., $[\alpha]^{25}_D$ +38 (*c* 0.1, MeOH)) was of similar sign and magnitude compared to that of compound **1**, suggesting that both molecules belong to the normal labdane series.

Vitexolide C (**4**) was isolated as colorless oil. Its molecular formula was established as $C_{20}H_{30}O_5$ from the pseudomolecular ion $[M + H]^+$ observed in HRESIMS spectrum (*m*/*z* 351.2185 calcd for 351.2166), which suggested the presence of an additional hydroxy group when compared with compounds **1**−**3**. The NMR spectroscopic data of compound **4** (^{13}C and ^{1}H chemical shifts and ^{1}H−^{1}H coupling constants) were similar on the one hand to those of **2** for the signals of the side chain and on the other hand to those of **3** for the signals corresponding to the decalin moiety. From these observations, hydroxy groups were positioned at C6 and C12. The relative configuration of compound **4** was established as 5*S**,6*R**,9*S**,10*R**,12*S**, and its absolute configuration should be the same as compound **2** at C12 and as compound **3** for the decalin moiety.

Vitexolin A (**5**) was isolated as a colorless oil and the molecular formula assigned as $C_{20}H_{32}O_3$ from its ^{13}C NMR

DOI: 10.1021/acs.jnatprod.5b00206
J. Nat. Prod. 2015, 78, 1348−1356

Table 2. ^{1}H NMR Data of Compounds 1−4 and 8 in Acetone-d_6

	1 500 MHz at 298 K	2 500 MHz at 298 K	3 600 MHz at 273 K	4 600 MHz at 243 K	8 500 MHz at 298 K
position	δ_H (J in Hz)	δ_H (J in Hz)	δ_H (J in Hz)	δ_H (J in Hz)	δ_H (J in Hz)
1α	1.11 td (13.0, 3.8)	1.15 td (13.0, 3.2)	1.08 m[a]	1.08 m[a]	1.11 td (12.7, 3.9)
1β	1.73 m[a]	1.76 m[a]	1.77 m[a]	1.66−1.82 m[a,b]	1.75 dt (12.7, 3.9)
2α	1.48 m	1.48 m	1.47 m	1.40−1.47 m[a,b]	1.49 m
2β	1.60 qt (13.8, 2.8)	1.60 qt (13.5, 3.2)	1.67 qt (14.0, 3.3)	1.61 m[a]	1.60 qt (13.8, 3.1)
3α	1.22 td (13.3, 3.8)	1.22 m[a]	1.19 td (13.2, 3.6)	1.18 m[a]	1.23 m[a]
3β	1.40 *br* d (13.3)	1.40 m[a]	1.31 *br* d (13.2)	1.28 m[a]	1.41 *br* m[a]
5	1.21 m[a]	1.21 m[a]	1.13 *br* s	1.13 *br* s[a]	1.21 dd (12.6, 2.1)
6α	1.36 qd (13.0, 4.0)	1.34 qd (12.5, 4.0)	4.42 *br* m	4.40 *br* m,	1.36 qd (12.7, 3.9)
6β	1.78 dt (13.0, 2.3)	1.76 m[a]			1.78 m[a]
OH6			3.19 d (3.7)	3.48 d (3.7)	
7α	2.03 m[a]	2.03 td (12.5, 5.2)	2.30 dd (13.4, 2.6)	2.28 *br* m	2.03 m[a]
7β	2.41 ddd (12.6, 4.0, 2.3)	2.41 ddd (12.5, 4.0, 2.3)	2.36 *br* d (13.4)	2.32 *br* m	2.42 ddd (12.7, 3.9, 1.9)
9	2.25 *br* d (11.3)[b]	1.88 m[a]	1.77 m[a]	1.77−1.84 d (10.7)[b]	2.21 td (5.7, 1.5)
11a	1.69 *br* t (12.9)[b]	1.88 m[a]	1.77−1.90 m[a,b]	1.91 m[b]	1.80 m
11b	1.90 t (12.9)[b]	2.08 m[a]	1.77−1.90 m[a,b]	2.10 m[b]	1.80 m
12	4.56 *br* d (10.6)[b]	4.61 *br* s[b]	2.20−2.30[a]	4.65−4.50 dd (8.5, 3.0)[b]	4.60 m
			2.50−2.60 m[a]		
14	6.05 s[b]	5.96 s	5.95−5.98 s[b]	5.95−6.04[b]	5.97 s
16	6.44[b] s	6.27 s	6.07−6.12 s[b]	6.28−6.23 s[b]	4.96 s
17a	4.67 d (1.2)	4.72 d (1.2)	4.71−4.74 s[b]	4.85−4.84 s[b]	4.54 d (1.2)
17b	4.87 d (1.2)	4.87 d (1.2)	4.90 s	4.87 s	4.87 d (1.2)
18	0.83 s	0.82 s	1.21 s	1.19 s	0.83 s
19	0.90 s	0.88 s	0.97 s	0.94 s	0.90 s
20	0.72 s	0.73 s	1.05 s	1.02−1.03 s	0.73 s

[a]Overlapped. [b]Broad or doubled signals.

Table 3. ^{13}C NMR Data of Compounds 1−4 and 8 in Acetone-d_6

position		1 125 MHz at 298 K	2 125 MHz at 298 K	3 150 MHz at 273 K	4 150 MHz at 243 K	8 125 MHz at 298 K
	type	δ_C (ppm)	δ_C (ppm)	δ_C (ppm)	δ_C (ppm)	δ_C (ppm)
1	CH_2	39.7	39.7	41.8	41.50−41.65[b]	39.7
2	CH_2	20.1	20.1	20.1	20.0	20.1
3	CH_2	43.0	42.9	44.5	44.4	43.0
4	C	34.5	34.2	34.9	34.9	34.3
5	CH	56.4	56.2	57.7−57.56[b]	57.3−57.5[b]	56.4
6	CH_2	25.3	25.3			25.3
	CH			68.9	68.9−68.8[b]	
7	CH_2	39.1	39.0	48.4	48.3	39.0
8	C	149.4	150.1	145.3−145.4[b]	146.1	149.5
9	CH	52.8	53.3	57.6−57.4[b]	53.3	52.8
10	C	40.2	40.7	41.4−41.5[b]	41.43−41.48[b]	40.1
11	CH_2	31.3	31.9	21.4−21.5[b]	31.7−31.3[b]	32.1
12	CH_2			27.1−27.2[b]		
	CH	66.6	67.9[b]		67.8−65.6[b]	67.3
13	C	171.1[b]	171.1[b]	171.6[b]	171.1−171.5[b]	176.3
14	CH	118.1[b]	118.0[b]	117.0−117.3[b]	117.6−117.5[b]	114.2
15	C	172.0[b]	172.0[b]	172.0[b]	173.2	174.1
16	CH_2					71.8
	CH	98.2[a]	99.3	99.5−100[b]	98.8−98.9[b]	
17	CH_2	107.4	107.2	109.1	109.2−109.0[b]	107.1
18	CH_3	22.1	22.2	24.0	23.9−24.0[b]	22.1
19	CH_3	34.1	34.0	33.9	33.8	34.0
20	CH_3	15.2	14.9	17.1	17.1−17.0[b]	15.2

[a]Signal observed on the spectrum performed at 263 K. [b]Broad or doubled signals.

data and the pseudomolecular ion $[M + H]^+$ at m/z 321.2410 (calcd for 321.2424) in HRESIMS, indicating five indices of hydrogen deficiency. Its IR spectrum shows evidence of an *exo*-methylene (ν_{max} 2927 and 890 cm^{-1}), an α,β-unsaturated

DOI: 10.1021/acs.jnatprod.5b00206
J. Nat. Prod. 2015, 78, 1348−1356

Table 4. ^{1}H and ^{13}C NMR Data of Compounds 5 and 6

	5 150 and 600 MHz at 298 K in $(CD_3)_2CO$		6 75 and 300 MHz at 298 K in $CDCl_3$	
position	δ_C	δ_H, mutiplicity (J in Hz)	δ_C	δ_H, multiplicity (J in Hz)
1α	39.5	0.94 td (13.1, 4.0)	39.5	1.08 td (13.1, 3.8)
1β		1.73 m[a]		1.52 m[a]
2α	19.9	1.46 m		1.43 m[a]
2β		1.58 qt (13.7, 3.2)	19.5	1.55 m[a]
3α	42.5	1.17 td (13.4, 3.7)	42.2	1.17 m[a]
3β		1.35 dt (13.4, 2.8)		1.40 m[a]
4	34.1		33.2	
5	56.0	1.09 dd (12.5, 2.6)	55.3	1.22 m[a]
6α	25.0	1.72 m[a]		1.74 m (12.4, 5.5, 2.4)
6β		1.29 qd (12.8, 3.9)	24.2	1.30 qd (12.4, 3.9)
7α	38.8	1.92 td (12.8, 5.0)	37.7	2.12 td (12.9, 5.5)
7β		2.37 ddd (12.8, 3.9, 2.2)		2.37 ddd (12.9, 3.9, 2.4)
8	149.3		149.3	
9	53.2	1.47 dt (13.7, 3.2)	51.5	2.53 *br* d (9.9)
10	39.9		39.2	
11	29.7	1.66 m[a]	33.2	2.68 dd (17.3, 3.6)
		1.74 m[a]		3.00 dd (17.3, 9.9)
12	76.3	4.14 dd (10.0, 4.3)	200.7	
13	161.5		142.2	
14	117.1	5.60 *br* s	37.5	3.25 d (16.5)
				3.32 d (16.5)
15	167.8		176.1	
16	12.7	2.08 d (1.0)	127.1	5.95 s
				6.25 s
17	107.2	4.68 d (1.2)	106.6	4.25 s
		4.86 d (1.2)		4.68 s
18	22.0	0.78 s	22.0	0.80 s
19	33.8	0.84 s	33.8	0.87 s
20	14.9	0.69 s	15.0	0.72 s

[a]Overlapped.

carboxylic acid (ν_{max} 1693 and 1647 cm^{-1}), and hydroxy groups (ν_{max} 3390 cm^{-1}). Analysis of 1D and 2D NMR data (Table 4) permitted identification of the unsubstituted labdane skeleton and evidenced one deshielded methyl group (δ_C 12.7/δ_H 2.08, $CH_3$16), an olefinic methine (δ_C 117.1/δ_H 5.60, CH14), an oxygenated methine (δ_C 76.3/δ_H 4.13, CH12), and a carboxylic group (δ_C 167.8, C15) on the side chain. The structure of the aliphatic side chain as depicted in Figure 2 and its attachment at C9 were deduced from HMBC correlations of $CH_3$16 to C12, C13, C14, and C15 as well as from $^{1}H-^{1}H$ COSY correlations of H9/H11 and H11/H12. The *E*-configuration of the double bond was confirmed by the absence of any ROESY correlation between $CH_3$16 and H14. The configuration at C12 of vitexolin A, also named 12-hydroxyanticopalic acid, remained unknown.

Vitexolin B (**6**) was isolated as a yellow oil. It possessed the molecular formula $C_{20}H_{30}O_3$, on the basis of its protonated molecular ion peak $[M + H]^+$ at m/z 319.2276 obtained by HRESIMS (calcd for 319.2268), corresponding to six indices of hydrogen deficiency. Its IR spectrum showed characteristic absorption bands accounting for exomethylenes (2933 and 885 cm^{-1}), enone and carboxylic acid (1713, 1683 and 944 cm^{-1}) functionalities. The specific rotation was established as $[\alpha]^{25}_D$ −20 (c 0.1, $CDCl_3$). Comparison of the NMR spectra of compound **6** with those of **5** (Table 4), revealed that the compounds differ in the substitution pattern of the side chain. Indeed, signals corresponding to one exomethylene at δ_C 127.1/δ_H 5.95/6.25 and 142.2 ($CH_2$16 and C13), one carbonyl at δ_C 200.7 (C12), and one methylene group at δ_C 37.5/δ_H 3.25/3.32, d, 16.5 Hz ($CH_2$14) were observed in the NMR spectra of **6**, whereas those of **5** displayed two ethylenic carbons, one oxymethine, and a methyl group. In compound **6**, these carbons can be connected as shown in Figure 2, through HMBC correlations from $H_2$14 to C12, C13, C15, and C16 and from $H_2$11 to C12 and C13 and C16. The side chain was positioned at C9 on the basis of the $^{1}H-^{1}H$ COSY correlation of H9 with H11. The relative configuration of compound **6**, which is the same as vitexolide A (**1**), was established as 5*S**,9*S**,10*S**.

Vitexolide E (**8**) was obtained as white powder. Its molecular formula was established as $C_{20}H_{30}O_3$ from the $[M + H]^+$ ion peak at m/z 319.2296 (calcd for $C_{20}H_{31}O_3$ 319.2268) in the HRESIMS spectrum. Its 1D and 2D NMR data were similar to those of 12-hydroxylabda-8(17),13-dien-15,16-olide isolated from *Turraeanthus manii* by Vardamides et al.,[22] which possesses the same molecular formula as **8**. However, the chemical shift value of H9 was different: δ_H 2.21 for **8** and δ_H 1.58 for the aforementioned known compound. Such a highfield shift of H9 was also observed for compound **1** compared to **2**, suggesting inversion of the configuration at C12. The absolute configuration remained undetermined for 12-hydroxylabda-8(17),13-dien-15,16-olide. Considering that the chemical shift value of H9 for compound **8** is similar to that in compound **1** (δ_H 2.25), it can be inferred that compounds **8** and **1** share the same relative and absolute

DOI: 10.1021/acs.jnatprod.5b00206
J. Nat. Prod. 2015, 78, 1348−1356

Table 5. MICs (μM) of Active Compounds and Reference Antibiotics

		compounds						antibiotics[b]				
bacterial species[a]	strain reference	**1**	**2**	**6**	**7**	**8**	**9**	AM	GM	CP	VA	OF
B. cereus	CIP 6624	12	24	50	50	≤188	46	11	1	6	0.3	0.7
	N190[c]	6	24	25	25	≤188	23	44	1	6	0.3	0.7
	N258[c]	6	24	50	25	≤188	46	11	2	6	0.3	0.7
	N349[c]	6	24	50	25	≤188	46	11	2	6	0.6	1.4
B. subtilis	ATCC 66.33	6	12	100	25	>188	46	≤0.2	0.3	12	0.1	≤0.2
C. striatum	N840[c]	24	96	158	50	>188	>46	350	>278	50	0.3	>354
E. avium	CIP 104 053	48	96	>158	>79	>188	>46	0.7	2	12	0.3	6
E. casseliflavus	N487[c]	96	>96	>158	>79	>188	>46	0.7	9	25	2.7	11
	CIP 103.018	96	>96	>158	>79	>188	>46	0.7	9	25	2.7	11
E. durans	CIP 104 999	24	48	>158	50	50	>46	1.4	17	12	0.3	1.4
E. faecalis	CIP 103.214	96	>96	>158	>79	50	>46	1.4	35	25	1.3	3
	CIP 104 676	24	96	>158	>79	50	>46	1.4	>278	200	5	3
	N491[c]	24	96	>158	>79	50	>46	0.7	>278	12	>86	6
	N518[c]	96	>96	>158	>79	50	>46	0.7	70	25	0.6	11
	N520[c]	48	96	>158	>79	50	>46	3	>278	200	0.6	354
E. faecium	CIP 103.014	96	>96	>158	>79	>188	>46	0.7	17	25	0.3	22
	CIP 107.387	96	>96	>158	>79	>188	>46	175	>278	12	>86	177
	N490[c]	48	>96	158	50	≤188	>46	22	>278	12	22	6
	N507[c]	96	>96	>158	>79	50	>46	350	>278	25	0.6	354
	N733[c]	96	>96	>158	>79	50	>46	>350	>278	12	>86	>354
	N823[c]	96	>96	>158	>79	50	>46	350	>278	25	>86	354
E. gallinarum	CIP 105 985	96	>96	>158	>79	>188	>46	1.4	17	12	5	11
	N489[c]	24	96	158	50	>188	>46	0.7	4	12	5	6
	N492[c]	48	96	>158	>79	>188	>46	0.7	17	25	5	11
E. hirae	CIP 5855	96	>96	>158	>79	>188	>46	1.4	35	12	0.3	3
L. innocua	E044[c]	48	>96	158	50	>188	>46	0.7	1	12	0.3	11
L. monocytogenes	CIP 103.575	24	96	158	>79	>188	>46	0.7	1	25	0.3	6
	N783[c]	48	96	158	50	>188	>46	0.7	1	12	0.3	6
	N836[c]	24	96	>158	50	>188	>46	0.7	1	12	0.3	6
	N851[c]	48	96	158	50	>188	>46	0.7	1	25	0.3	6
S. aureus	ATCC 25.923	24	48	158	>79	>188	>46	0.3	1	25	0.6	1.4
	ATCC 9144 Oxford	24	48	158	50	>188	>46	≤0.2	0.5	12	0.2	0.7
	CIP 4.83	12	48	158	>79	>188	>46	0.3	1	12	0.6	0.7
	CIP 53154	24	48	158	50	>188	>46	0.3	4	12	0.6	0.7
	CIP 53156	12	48	158	50	>188	>46	≤0.2	1	12	0.3	0.7
	CIP 5710	24	48	100	>79	>188	>46	0.7	1	12	0.6	0.7
	CIP 7625	24	48	158	>79	>188	>46	0.3	1	25	2.7	1.4
	CRBIP 21.21	12	48	100	50	>188	>46	175	>278	12	2.7	177
S. epidermidis	CIP 53.124	12	48	158	50	>188	>46	≤0.2	0.5	6	0.6	1.4
S. hemolyticus	CIP 81.56	6	24	158	>79	>188	>46	≤0.2	≤0.14	6	0.6	0.7
S. intermedius	N987[c]	12	24	100	50	>188	>46	88	139	25	0.6	89
S. lugdunensis	ATCC 43.809	24	48	158	79	>188	>46	0.7	0.5	12	0.6	3
S. saprophyticus	CIP 76125	24	48	158	>79	>188	>46	0.7	0.3	25	0.6	3
	E260[c]	24	48	158	>79	>188	>46	0.7	≤0.14	25	0.6	3
S. sciuri	N993[c]	48	96	158	>79	>188	>46	0.7	≤0.14	12	0.6	3
St. agalactiae	CIP 103.227	12	24	100	50	50	>46	≤0.2	2	3	0.3	1.4

[a]Bacterial species: *B* = *Bacillus*, *C* = *Corynebacterium*, *E* = *Enterococcus*, *L* = *Listeria*, *S* = *Staphylococcus*, *St* = *Streptococcus*. [b]AM = amoxicillin, GM = gentamicin, CP = chloramphenicol, VA = vancomycin, OF = ofloxacin. [c]Clinical strains from the collection of Laboratoire Ecosystème Intestinal, Probiotiques, Antibiotiques-EA 4065.

configuration at C12 (12*R*) and consequently that the configuration at C12 of its epimer should be the same as that of **2** (i.e., 12*S*).

The antibacterial activities of compounds **1**−**10** were evaluated against 46 Gram-positive strains (minimal inhibitory concentration, MIC, are in μM in Table 5, and are in mg/L in Table 5a in Supporting Information). Compounds **3**−**5** and **10** showed no activity at tested concentrations. Compounds **6** and **9** were active on four out of five and all five *Bacillus* strains with MICs between 23 and 50 μM. Vitexolide E (**8**) was active at 50 μM against 10 strains (among them, three strains were resistant to vancomycin): all five *Enterococcus faecalis*, three out of six *Enterococcus faecium*, one *Enterococcus durans*, and one *Streptococcus agalactiae*. Vitexolide D (**7**) inhibited four out of five *Bacillus* strains at 25 μM and 16 additional strains at 50 μM: the last strain of *Bacillus cereus*, one *Corynebacterium striatum*, three *Enterococcus* sp. (in which a strain of *E. faecium* is resistant to vancomycin), four out of five *Listeria* sp., four out of

DOI: 10.1021/acs.jnatprod.5b00206
J. Nat. Prod. 2015, 78, 1348−1356

eight *Staphylococcus aureus* (in which the multiresistant reference strain is CRBIP 21.21), two out of seven other *Staphylococcus*, and one *Streptococcus agalactiae*. Vitexolide A (**1**), and to a lesser extent 12-epivitexolide A (**2**), showed potent antibacterial activity on the same strains. The most active compound was vitexolide A (**1**) because MICs of compound **2** were 2 or 4 times higher. At 48 μM or less, this compound inhibited 35 out of 46 strains, whereas at 96 μM all strains were inhibited. The more sensitive species were: *Bacillus* sp. (MIC = 6−12 μM), *Staphylococcus* sp. (MIC = 6−24 μM except *S. sciuri*), and *Streptococcus agalactiae* (MIC = 12 μM).

The cytotoxicities of compounds **1**−**4** and **6**−**9** were also evaluated at two concentrations in the range of their bactericidal activity (1 and 10 μM) against a human colon cancer carcinoma cell line (HCT-116) and on a human fetal lung fibroblast cell line (MRC5). As shown in Table 6, all

Table 6. Evaluation of the Cytotoxicity of Compounds 1−4 and 6−9

	MRC5% of cytotoxicity		HCT-116% of cytotoxicity	
	10^{-5} M (~3 mg/L)	10^{-6} M (~0.3 mg/L)	10^{-5} M (~3 mg/L)	10^{-6} M (~0.3 mg/L)
1	95	22	87	0
2	67	19	90	1
3	28	5	38	0
4	0	0	66	0
6	25	22	46	0
7	71	0	69	0
8	86	34	68	3
9	92	29	84	0

compounds inhibited more or less strongly the growth of HCT-116 cells at a concentration of 10 μM but were not cytotoxic at 1 μM. A similar cytotoxic effect was measured against MRC5 cells, with the exception of compounds **3**, **4**, and **6**, which exhibit weak or no cytotoxicity at both concentrations. Compounds **8** and **9**, and to a lesser extent compounds **4**, **6**, and **7**, were cytotoxic albeit devoid of any significant antibacterial activity. These data indicated that different mechanisms of action could be involved in the activities reported herein for these compounds.

According to these results and literature data, a preliminary structure−activity relationship could be drawn. The C12 epimers **1** and **2** are both active on a broad spectrum of Gram-positive bacteria. Nyiligira and co-workers reported a similar activity for an *ent*-labdane isolated from a *Vitex* species having the same side chain as **2**.[23] Thus, it seems that the presence of a γ-hydroxybutenolide moiety, together with a C12 hydroxy group, contributed to high bactericidal activity. Because compound **1** is slightly more active than **2**, the 9*S*-12*R* stereochemistry is likely beneficial to the antibacterial activity. In addition, because compounds **3** and **4** are inactive, a 6βOH group is likely deleterious for bactericidal activity. The replacement of the γ-hydroxybutenolide moiety (**1**) by a butenolide (**8**) resulted in a complete loss of biological activity on *Staphylococcus*, *Listeria*, and *Bacillus* strains, whereas the activities on *Enterococcus faecalis* and *E. faecium* are slightly improved. This observation suggested that the bactericidal activity against *Enterococcus* could be mediated by a different mechanism of action than for other Gram-positive bacteria. The bactericidal mode of action of labdane diterpenoids on *Staphylococcus aureus* was recently explored by Ghosh.[24] The author confirmed that these compounds were responsible for bacterial cell membrane damage and disintegration.

The phytochemical investigation of *Vitex vestita* led to the isolation of six new labdane derivatives (**2**−**6** and **8**) along with six known compounds (**1**, **7**, and **9**−**12**). Vitexolide A (**1**) and 12-epivitexolide A (**2**) were found to be the most promising candidates for further development. The structure−activity relationship analysis suggested that the presence of the γ-hydroxybutenolide moiety together with a C12 hydroxylation contributed to its bactericidal activity. Further studies are needed for a better understanding of their antibacterial mechanisms of action.

EXPERIMENTAL SECTION

General Experimental Procedures. Optical rotations were determined at 25 °C with a JASCO P1010 polarimeter. UV spectra were recorded using a PerkinElmer Lambda 5 spectrophotometer. IR spectra were measured on a Nicolet FT-IR 205 spectrophotometer. The 1D and 2D NMR Data were recorded in acetone-d_6 and $CDCl_3$ on a Bruker Avance 600 MHz instrument for compounds **3**−**5**, a Bruker Avance 300 MHz instrument for **6**, and on a Bruker Avance 500 MHz instrument for compounds **1**, **2**, and **8**. High resolution MS data were obtained using an UPLC system coupled to a Waters LCT Premier XE mass spectrometer equipped with an electrospray ionization source. The ionization was carried out in positive mode in the 80−1500 *m*/*z* range. UPLC was performed with an Acquity Waters UPLC system equipped with a Waters Acquity PDA dectector. The wavelength range was between 210 and 410 nm. Separations were done on a BEH C_{18} column (50 mm × 2.1 mm, 1.7 μm, Waters) at a flow rate of 0.6 mL/min. Elution was conducted with a H_2O/0.1% HCO_2H−MeCN/0.1% HCO_2H gradient as follows: 95:5−0:100 in 5.5 min. A Kromasil C_{18} column, (250 mm × 4.5 mm, 5 μm, Thermo) was used for analytical HPLC separation using a Waters alliance system equipped with a binary pump (Waters 2525), a UV−vis diode array detector (190−600 nm, Waters 2996), and a PL-ELS 1000 ELSD Polymer Laboratory detector. This system was also used in preparative mode (disconnected from ELSD) to purify small amounts of products. A Kromasil C_{18} column (250 mm × 10 mm, 5 μm, Thermo) was used for preparative HPLC separation using a Dionex autopurification system equipped with a binary pump (P580), a UV−vis array detector (200−600 nm, Dionex UVD340U), and a PL-ELS 1000 ELSD detector Polymer Laboratory. Prepacked silica cartridges were used for flash chromatography using a Combiflash-Companion apparatus (Serlabo). Analytical TLC plates (Si gel 60 F 254) were purchased from SDS (France).

Plant Material. The leaves of *V. vestita* were collected in November 2008 in Machang district, Kelantan state, Malaysia. The plant was identified by T. Leong Eng, Botanist, University of Malaya. A voucher specimen (KL-5600) has been deposited at the herbarium of the Department of Chemistry, Faculty of Sciences, University of Malaya, Kuala Lumpur, Malaysia.

Preparation of Plant Extracts for Large-Scale in Vitro Antibacterial Screening. A 50 g portion of air-dried and powdered different parts of 476 tropical plants have been extracted with MeOH using an accelerated solvent extractor (heating at 40 °C for 5 min, 100 bar, 3 cycles) to give 1−10 g of 869 crude extracts. These extracts (approximately 30 mg) were dissolved with a small volume of CH_2Cl_2 to constitute a batch of 1392 organic extracts (869 MeOH and 523 CH_2Cl_2 extracts). They were tested on a panel of 49 bacterial strains representing 41 species (15 Gram-positive and 26 Gram-negative). From the 1392 organic extracts, only six extracts from five species (two MeOH and four CH_2Cl_2) were shown to have potent antibacterial activities (defined as inhibition of several bacterial species and/or one pathogen species).

Extraction and Isolation. The air-dried and powdered leaves of *V. vestita* (480 g) were extracted with CH_2Cl_2 (3 × 4.0 L, 1 h each, 40 °C, 100 bar) using a Zippertex static high-pressure, high-temperature extractor, to yield 14.1 g of crude extract after evaporation in vacuo at

DOI: 10.1021/acs.jnatprod.5b00206
J. Nat. Prod. 2015, 78, 1348−1356

40 °C. A portion (7 g) of this extract was subjected to flash column chromatography on silica gel eluted with heptane followed by a CH_2Cl_2/EtOAc/MeOH gradient (1:0:0−0:1:0−0:5:5) at 40 mL/min leading to 16 fractions, F1−F16, according to their TLC profiles. The active fraction F9 (2.25 g) was subjected to flash column chromatography on silica gel using a CH_2Cl_2/EtOAc/MeOH gradient (1:0:0−0:1:0−0:5:5) at 30 mL/min to obtain 11 subfractions of increasing polarity (F_{9-1}−F_{9-11}). The purification of the subfractions was performed on a preparative Kromasil C_{18} column (250 mm × 10 mm, 5 μm) using MeCN/H_2O + 0.1% HCO_2H as eluant (proportion annotated X:X in the following part) in isocratic mode at 17 mL/min. The purification of F_{9-5} (200 mg) afforded compound **1** (36 mg) (55:45, t_R = 33.5 min). The purification of F_{9-6} (140 mg) afforded compounds **2** (32 mg), **5** (8 mg), and **10** (2 mg) (60:40, t_R = 21.4, 26.8, and 14.3 min, respectively). The purification of F_{9-2} (82 mg) led to compounds **12** (4 mg), **7** (4 mg), **8** (6 mg), and **6** (20 mg) (75:25, t_R = 10.9, 13.1, 15.5, and 17.5 min, respectively). The purification of F_{9-4} (150 mg) yielded compound **3** (20 mg) (60:40, t_R = 13.2 min). The purification of F_{9-8} (90 mg) afforded compounds **4** (5 mg) and **9** (11 mg) (65:35, t_R = 6.0 and 9.4 min respectively). The purification of F_{9-7} (271 mg) led to compound **11** (3 mg) (60:40, t_R = 28.0 min).

*Vitexolide A (**1**), (12R,16ζ)-12,16-dihydroxylabda-8(17),13-dien-15-16-olide:* white powder; $[\alpha]^{25}_D$ +46 (*c* 0.05, MeOH); UV (MeOH) λ_{max} (log ε) 208 (4.43) nm; IR ν_{max} 3340, 2938, 1742, 1640, 890 cm^{-1}; ^1H and ^{13}C NMR Tables 2 and 3; HRESIMS *m*/*z* 335.2226 $[M + H]^+$ (calcd for $C_{20}H_{31}O_4$, 335.2217).

*12-Epivitexolide A (**2**), (12S,16ζ)-12,16-dihydroxylabda-8(17),13-dien-15−16-olide:* colorless oil; $[\alpha]^{25}_D$ −2 (*c* 0.1, MeOH) ; UV (MeOH) λ_{max} (log ε) 208 (4.43) nm; IR ν_{max} 3370, 2932, 1746, 1644, 890 cm^{-1}; ^1H and ^{13}C NMR Tables 2 and 3; HRESIMS *m*/*z* 335.2220 $[M + H]^+$ (calcd for $C_{20}H_{31}O_4$, 335.2217).

*Vitexolide B (**3**), (6R,16ζ)-6,16-dihydroxylabda-8(17),13-dien-15−16-olide:* white powder; $[\alpha]^{25}_D$ +38 (*c* 0.1, MeOH); UV (MeOH) λ_{max} (log ε) 208 (4.06) nm; IR ν_{max} 3386, 2928, 1720, 1642, 920 cm^{-1}; ^1H and ^{13}C NMR Tables 2 and 3; HRESIMS *m*/*z* 335.2223 $[M + H]^+$ (calcd for $C_{20}H_{31}O_4$, 335.2217).

*Vitexolide C (**4**), (6R,12S,16ζ)-6,12,16-trihydroxylabda-8(17),13-dien-15−16-olide:* colorless oil; $[\alpha]^{25}_D$ +4 (*c* 0.1, MeOH); UV (MeOH) λ_{max} (log ε) 210 (4.36) nm; ^1H and ^{13}C NMR Tables 2 and 3; HRESIMS *m*/*z* 351.2185 $[M + H]^+$ (calcd for $C_{20}H_{31}O_5$, 351.2266).

*Vitexolin A (**5**), (12ζ)12-hydroxylabda-8(17)-13(E)-dien-15-oic acid:* white powder; $[\alpha]^{25}_D$ +21 (*c* 0.1, MeOH); UV (MeOH) λ_{max} (log ε) 208 (3.81) nm; IR ν_{max} 3390, 2927, 1693, 1647, 890 cm^{-1}; ^1H and ^{13}C NMR Table 4; HRESIMS *m*/*z* 321.2410 $[M + H]^+$ (calcd for $C_{20}H_{33}O_3$, 321.2424).

*Vitexolin B (**6**), 12-oxo-labda-8(17),13(16)-dien-15-oic acid:* yellow oil; $[\alpha]^{25}_D$ −22 (*c* 0.1, $CHCl_3$); UV ($CHCl_3$) λ_{max} (log ε) 233 (10.3) nm; IR ν_{max} 2933, 1713, 1683, 884 cm^{-1}; ^1H and ^{13}C NMR Table 4; HRESIMS *m*/*z* 319.2276 $[M + H]^+$ (calcd for $C_{20}H_{31}O_3$, 319.2268).

*Vitexolide D (**7**), (12S)-12-hydroxylabda-8(17),13-dien-15−16-olide:* white powder; $[\alpha]^{25}_D$ +3 (*c* 0.1, $CHCl_3$), lit. $[\alpha]^{22}_D$ +3.6 (*c* 0.3, $CHCl_3$); HRESIMS *m*/*z* 319.2269 $[M + H]^+$ (calcd for $C_{20}H_{31}O_3$, 319.2268); ^1H and ^{13}C NMR data are comparable to published data.[11]

*Vitexolide E (**8**), (12R)-12-hydroxylabda-8(17),13-dien-15−16-olide:* white powder; $[\alpha]^{25}_D$ +16 (*c* 0.1, $CHCl_3$); UV ($CHCl_3$) λ_{max} (log ε) 234 (10.6) nm; ^1H and ^{13}C NMR Tables 2 and 3; HRESIMS *m*/*z* 319.2296 $[M + H]^+$ (calcd for $C_{20}H_{31}O_3$, 319.2268).

X-ray Crystallographic Analysis. X-ray crystallographic data were collected on a Rigaku diffractometer constituted by am MM007 HF copper rotating-anode generator, equipped with Osmic confocal optics and a Rapid II curved Image Plate. Crystal data of **1**: $C_{20}H_{30}O_4$, *M* = 334.44, needle-like crystal, size = 0.10 mm × 0.09 mm × 0.06 mm, orthorhombic, space group $P2_12_12_1$, *a* = 7.4701(9) Å, *b* = 9.9307(15) Å, *c* = 24.744(4) Å, $\alpha = \beta = \gamma = 90°$, *V* = 1835.6(5) $Å^3$, *T* = 293(2) K, *Z* = 4, *d* = 1.210 g/cm3, λ(Cu Kα) = 1.54187 Å, *F*(000) = 728, reflections collected/unique = 15785/3330 [$R_{(int)}$ = 0.0994], *h* (−9/8), *k* (−11/11), *l* (−25/29), theta range = 3.57−68.24°, completeness = 99.8%, data/restraints/parameters = 3330/0/220, final *R* indices: R_1 = 0.0837 and wR_2 = 0.1988 ($I > 2\sigma(I)$), R_1 = 0.1544 and wR_2 = 0.2467 (all data), GOF = 0.975, largest diff. peak and hole = 0.281 and −0.224 e·$Å^{-3}$; absolute structure parameter = 0.4(3) using 409 quotients.[25]

Crystallographic data for **1** have been deposited with the Cambridge Crystallographic Data Centre (deposit no. CCDC 1043902). Copies of the data can be obtained, free of charge, on application to the Director, CCDC, 12 Union Road, Cambridge CB2 1EZ, United Kingdom (fax: +44-(0)223-336033 or e-mail: deposit@ccdc.cam.ac.uk).

Preparation of Acetylated Derivatives of Compounds 1 and 2. Compound **1** (5 mg) was stirred at room temperature with Ac_2O (0.5 mL) and pyridine (1 mL) for 24 h. The solvents were removed under reduced pressure. The ^1H NMR spectrum of the residue revealed a mixture of two diacetylated compounds in a 2:1 ratio. The residue (3.5 mg) was subjected to HPLC using a Nucleodur-PFP analytical column (250 mm × 4.6 mm, 5 μm, Macherey-Nagel) eluted with MeCN/H_2O (60:40 + 0.1% HCO_2H) to afford 1.3 mg of **1a** (t_R = 23.09 min) and 0.6 mg of **1b** (t_R = 24.69 min). Compound **2** (5 mg) was acetylated using the same procedure as for **1**. The ^1H NMR spectrum of the residue revealed a mixture of two diacetylated compounds in a 1:1 ratio. Purification of the residue (2 mg) was performed using a Hypercarb analytical column (150 mm × 4.6 mm, 5 μm, Thermo) with MeCN/H_2O (70:30 + 0.1% HCO_2H) as eluent to afford 0.6 mg of **2a** (t_R = 21.66 min) and 0.6 mg of **2b** (t_R = 24.34 min).

Bacterial Assay. The in vitro antibacterial bioassay was conducted using an agar-dilution method with ofloxacin as the positive control. Extracts, fractions, and compounds were dissolved in DMSO. Extracts and fractions were tested at the concentration of 60 mg/L. For determination of the MIC, geometric dilutions were prepared in DMSO to give final concentrations of 100−0.75 mg/L. Then, 250 μL of the solutions were incorporated in Mueller Hinton agar (BioMérieux) to a final volume of 20 mL. Each strain was incubated for 18 h at 37 °C in trypticase soy broth (BioMérieux). Cultures were diluted in sterile distilled H_2O and applied on test medium using a Steers inoculator; inoculum was about 1000 UFC/spot. Test media were incubated for 18 h at 37 °C. The blank controls of microbial cultures were incubated with 250 μL DMSO under the same conditions. DMSO was determined to be nontoxic under these conditions. The MIC was recorded as the lowest concentration at which no bacterial growth was observed. MICs of amoxicillin, gentamicin, chloramphenicol, and vancomycin were determined for comparison. A panel of 49 strains (30 Gram-negative and 19 Gram-positive representing, respectively, 26 and 15 species) were used for screening of crude extracts and bioguiding. A panel of 46 Gram-positive strains representing 20 species, selected on the basis of the results of screening, was used to test compounds.

Cell Culture and Proliferation Assay. Cell lines were obtained from the American Type Culture Collection (Rockville, MD, USA) and were cultured according to the supplier's instructions. Human HCT-116 colorectal carcinoma cells were grown in RPMI 1640 supplemented with 10% fetal calf serum (FCS) and 1% glutamine, and the human MRC5 cells derived from normal lung tissue were grown in DMEM supplemented with 10% FCS and 1% glutamine. Cell lines were maintained at 37 °C in a humidified atmosphere containing 5% CO_2. Cell growth inhibition was determined by an MTS assay according to the manufacturer's instructions (Promega, Madison, WI, USA). Briefly, the cells were seeded in 96-well plates (2.5 × 10^3 cells/well) containing 200 μL of growth medium. After 24 h of culture, the cells were treated with the tested compounds at 1 and 10 μM final concentrations. After 72 h of incubation, 40 μL of resazurin was added 2 h before recording absorbance at 490 nm with a spectrophotometric plate reader. The percent cytotoxicity index (($OD_{490treated}/OD_{490control}$) × 100) was calculated from three experiments.

DOI: 10.1021/acs.jnatprod.5b00206
J. Nat. Prod. 2015, 78, 1348−1356

■ ASSOCIATED CONTENT

Supporting Information

^{1}H and ^{13}C NMR spectra, and HRESIMS data for compounds **2**−**6** and **8**, ORTEP views and a detailed discussion on X-ray structure determination for compound **1**, and crystallographic information file (CIF) for compound **1**, and MICs in mg/L of active compounds. The Supporting Information is available free of charge on the ACS Publications website at DOI: 10.1021/acs.jnatprod.5b00206.

■ AUTHOR INFORMATION

Corresponding Author

*Tel.: + 33 1 69 82 30 85. Fax: + 33 1 69 07 72 47. E-mail: marc.litaudon@cnrs.fr.

Notes

The authors declare no competing financial interest.

■ ACKNOWLEDGMENTS

This research was conducted within the context of the International French Malaysian Natural Product Laboratory (IFM-NatProLab). This work has benefited from an Investissement d'Avenir grant managed by Agence Nationale de la Recherche (CEBA, ANR-10-LABEX-25-01) and also from ANR-09-CP2D-09-01. This research was also supported by grants from the University Malaya (UM; UM.C/625/1/HIR/MOHE/SC/37). We express our thanks to the staff of the laboratory EA 4065 for technical assistance in the antibacterial assays, to N. Bourgeois-Nicolaos for providing vancomycin-resistant enterococci clinical strains, to D. M. Nor (UM), R. Syamsir (UM) and T. Leong Eng (UM) for the collection and identification of plant material, and to Mrs. H. Leveque (ICSN) who performed the cytotoxic assays.

■ REFERENCES

(1) De Kok, R. *Kew Bull.* **2008**, *63*, 17−40.
(2) Rani, A.; Sharma, A. *Pharmacogn. Rev.* **2013**, *7*, 188−198.
(3) Kannathasan, K.; Senthilkumar, A.; Venkatesalu, V. *Asian Pac. J. Trop. Med.* **2011**, *4*, 645−648.
(4) Ono, M.; Yanaka, T.; Yamamoto, M.; Ito, Y.; Nohara, T. *J. Nat. Prod.* **2002**, *65*, 537−541.
(5) Ono, M.; Yamamoto, M.; Masuoka, C.; Ito, Y.; Yamashita, M.; Nohara, T. *J. Nat. Prod.* **1999**, *62*, 1532−1537.
(6) Zheng, C.-J.; Zhu, J.-Y.; Yu, W.; Ma, X.-Q.; Rahman, K.; Qin, L.-P. *J. Nat. Prod.* **2013**, *76*, 287−291.
(7) Ono, M.; Nagasawa, Y.; Ikeda, T.; Tsuchihashi, R.; Okawa, M.; Kinjo, J.; Yoshimitsu, H.; Nohara, T. *Chem. Pharm. Bull.* **2009**, *57*, 1132−1135.
(8) Shul'ts, E. E.; Mironov, M. E.; Kharitonov, Yu. V. *Chem. Nat. Compd.* **2014**, *50*, 2−21.
(9) Sreedhar, V.; Ravindra Nath, L. K.; Madana Gopal, N.; Raju, D.; Venu Gopal, K.; Raja Sekhar, K. K. *J. Pharm. Res.* **2011**, *4*, 288−290.
(10) Villamizar, J. E.; Juncosa, J.; Pittelaud, J.; Hernández, M.; Canudas, N.; Tropper, E.; Salaza, F.; Fuentes, J. *J. Chem. Res.* **2007**, 342−346.
(11) Boukouvalas, J.; Wang, J.-X.; Marion, O.; Ndzi, B. *J. Org. Chem.* **2006**, *71*, 6670−6673.
(12) Ik-Soo, L.; Xianjian, M.; Hee-Byung, C.; Madulid, D. A.; Brian Lamont, R.; O'Neill, M. J.; Besterman, J. M.; Farnsworth, N. R.; Doel Soejarto, D.; Cordell, G. A.; Pezzuto, J. M.; Douglas Kinghorn, A. *Tetrahedron* **1995**, *51*, 21−28.
(13) Furuichi, N.; Hata, T.; Soetjipto, H.; Kato, M.; Katsumura, S. *Tetrahedron* **2001**, *57*, 8425−8442.
(14) Braun, S.; Breitenbach, H. *Tetrahedron* **1977**, *33*, 145−150.
(15) Cunningham, A.; Martin, S. S.; Langenheim, J. H. *Phytochemistry* **1974**, *13*, 294−295.
(16) Zdero, C.; Bohlmann, F.; King, R. M. *Phytochemistry* **1992**, *31*, 1631−1638.
(17) Valters, R. E.; Flitsch, W. *Ring-Chain Tautomerism*; Katritsky, A. R., Ed.; Plenum: New York, 1985; Vol. *1*. pp 19−38.
(18) Gunasekera, S. P.; McCarthy, P. J.; Kelly-Borges, M.; Lobkovsky, E.; Clardy, J. *J. Am. Chem. Soc.* **1996**, *118*, 8759−8760.
(19) Miles, W. H.; Duca, D. G.; Selfridge, B. R.; Palha De Sousa, C. A.; Hamman, K. B.; Goodzeit, E. O.; Freedman, J. T. *Tetrahedron Lett.* **2007**, *48*, 7809−7812.
(20) Zani, C. L.; Alves, T. M. A.; Queiroz, R.; Fontes, E. S.; Shin, Y. G.; Cordell, G. A. *Phytochemistry* **2000**, *53*, 877−880.
(21) Hong-Xi, X.; Hui, D.; Keng-Yeow, S. *Phytochemistry* **1996**, *42*, 149−151.
(22) Vardamides, J. C.; Sielinou, V. T.; Ndemangou, B.; Nkengfack, A. E.; Fomum, Z. T.; Poumale, H. M.; Laatsch, H. *Planta Med.* **2007**, *73*, 491−495.
(23) Nyiligira, E.; Viljoen, A. M.; Van Heerden, F. R.; Van Zyl, R. L.; Van Vuuren, S. F.; Steenkamp, P. A. *J. Ethnopharmacol.* **2008**, *119*, 680−685.
(24) Ghosh, S.; Indukuri, K.; Bondalapati, S.; Saikia, A. K.; Rangan, L. *Eur. J. Med. Chem.* **2013**, *66*, 101−105.
(25) Parsons, S.; Flack, H. *Acta Crystallogr.* **2004**, *A60*, s61.

DOI: 10.1021/acs.jnatprod.5b00206
J. Nat. Prod. 2015, 78, 1348−1356